AC

DESY 97-231
November 1997

Stop Mixing in the $\mathcal{MSSM}$

T. Plehn
Deutsches Elektronen-Synchrotron DESY, Hamburg
W. Beenakker
Instituut-Lorentz, University of Leiden, The Netherlands

ISSN 0418-9833

DESY 97-231
November 1997
ISSN 0418-9833

STOP MIXING IN THE $\mathcal{MSSM}$

T. Plehn

Deutsches Elektronen–Synchrotron DESY, D-22603 Hamburg

W. Beenakker

Instituut–Lorentz, University of Leiden, The Netherlands

Stop particles are expected to be the lightest squarks in the minimal supersymmetric standard model. The search for these particles is therefore an important experimental task at e^+e^- as well as at hadron colliders. The light mass of the $\tilde{t}_1$ particle is caused by strong mixing effects. We discuss a recently developed renormalization scheme for the associated mixing angle. In addition, we briefly present some features of the partial decay widths in the stop sector and the hadroproduction of stop pairs at the Tevatron/LHC in next-to-leading order (NLO) supersymmetric QCD (SUSY-QCD), including the dependence on the mixing angle.

1 Introduction

Within the squark sector of SUSY theories, the top-squark (stop) eigenstate $\tilde{t}_1$ is expected to be the lightest particle[1]. If the scalar masses in grand unified theories, for instance, are evolved from universal values at the GUT scale down to low scales, the $\tilde{t}_1$ top-squark drops to the lowest value in the squark spectrum. Moreover, the strong Yukawa coupling between top/stop and Higgs fields gives rise to large mixing, leading to a potentially small mass eigenvalue for $\tilde{t}_1$. In fact, the $\tilde{t}_1$ mass could be even smaller than the top-quark mass itself.

In e^+e^- and $p\bar{p}/pp$ collisions stop particles are produced in pairs. Present limits from LEP2 indicate a $\tilde{t}_1$ mass in excess of 67 GeV, independent of the mixing angle in the stop sector, but depending on the lightest neutralino mass[2]. Preliminary analyses at the Tevatron have led to a lower limit of 93 GeV for the $\tilde{t}_1$ mass, depending on the lightest neutralino mass[3]. In contrast to the case of e^+e^- colliders, where the mixing angle can be measured directly[4], the role of the mixing angle in the analysis of hadron collisions is less prominent, but may possibly influence the extraction of mass limits from the data.

2 Mixing-Angle Renormalization

The large Higgs–Yukawa coupling in the stop sector leads to potentially strong mixing in the symmetric stop mass matrix, which reads in the notation of Ref.[5]

$$\mathcal{M}^2 = \begin{pmatrix} m_Q^2 + m_t^2 + \left(\frac{1}{2} - \frac{2}{3}s_w^2\right) m_Z^2 \cos(2\beta) & -m_t\,(A_t + \mu\cot\beta) \\ -m_t\,(A_t + \mu\cot\beta) & m_U^2 + m_t^2 + \frac{2}{3}s_w^2 m_Z^2 \cos(2\beta) \end{pmatrix} \quad (1)$$

The diagonal elements of the stop mass matrix correspond to the left-chirality (L) and right-chirality (R) squark-mass terms, the off-diagonal elements are induced by the chirality-flip Yukawa interactions. These Yukawa interactions rotate the chiral states $\tilde{t}_{L0}$ and $\tilde{t}_{R0}$ into the mass eigenstates $\tilde{t}_{10}$ and $\tilde{t}_{20}$:

$$\begin{pmatrix} \tilde{t}_{10} \\ \tilde{t}_{20} \end{pmatrix} = \begin{pmatrix} \cos\tilde{\theta}_0 & \sin\tilde{\theta}_0 \\ -\sin\tilde{\theta}_0 & \cos\tilde{\theta}_0 \end{pmatrix} \begin{pmatrix} \tilde{t}_{L0} \\ \tilde{t}_{R0} \end{pmatrix} \quad (2)$$

The mass eigenvalues and the leading-order (LO) rotation angle can be expressed by the elements of the mass matrix.

SUSY-QCD corrections, involving only the stop and gluino ($\tilde{g}$) particles besides the usual particles of the Standard Model, modify the stop mass matrix and the stop fields. This gives rise to the renormalization of the masses and of the wave functions [$\tilde{t}_{i0} = Z_{ij}^{1/2}\,\tilde{t}_j$]. Motivated by the symmetry properties of the stop interactions, we choose a real wave-function renormalization matrix $Z^{1/2}$ that can be split into a real orthogonal matrix $\mathcal{R}(\delta\tilde{\theta})$ and a diagonal matrix $Z_{\text{diag}}^{1/2}$ [i.e. $Z^{1/2} = \mathcal{R}(\delta\tilde{\theta})\,Z_{\text{diag}}^{1/2}$]. The rotational part can be reinterpreted as a shift of the mixing angle[5,6], given by $\tilde{\theta}_0 - \delta\tilde{\theta} \equiv \tilde{\theta}$:

$$\begin{pmatrix} \tilde{t}_1 \\ \tilde{t}_2 \end{pmatrix} = \begin{pmatrix} 1/Z_{\text{diag},\,11}^{1/2} & 0 \\ 0 & 1/Z_{\text{diag},\,22}^{1/2} \end{pmatrix} \begin{pmatrix} \cos\tilde{\theta} & \sin\tilde{\theta} \\ -\sin\tilde{\theta} & \cos\tilde{\theta} \end{pmatrix} \begin{pmatrix} \tilde{t}_{L0} \\ \tilde{t}_{R0} \end{pmatrix} \quad (3)$$

This counterterm for the mixing angle allows a diagonalization of the real part of the inverse stop propagator matrix in any fixed-order perturbation theory:

$$\begin{aligned} \mathrm{Re}\left[D_{\text{ren}}^{-1}(p^2)\right] &= \left(Z^{1/2}\right)^T \left[p^2\,\mathbf{1} - \mathcal{M}^2 + \mathrm{Re}\,\Sigma(p^2)\right] \left(Z^{1/2}\right) \\ &= \left(Z_{\text{diag}}^{1/2}\right) D_{\text{diag}}^{-1}(p^2) \left(Z_{\text{diag}}^{1/2}\right) \end{aligned} \quad (4)$$

for $\tan(2\delta\tilde{\theta}) = 2\,\mathrm{Re}\,\Sigma_{12}(p^2)/[m_{\tilde{t}_1}^2 - m_{\tilde{t}_2}^2 + \mathrm{Re}\,\Sigma_{22}(p^2) - \mathrm{Re}\,\Sigma_{11}(p^2)]$. This holds as long as the unrenormalized stop self-energy matrix $\Sigma(p^2)$ is symmetric.

We fix the renormalization constants by imposing the following two conditions on the renormalized stop propagator matrix: (i) The diagonal elements should approach the form $1/D_{\text{ren},jj}(p^2) \to p^2 - m^2_{\tilde{t}_j} + i m_{\tilde{t}_j}\Gamma_{\tilde{t}_j}$ for $p^2 \to m^2_{\tilde{t}_j}$, with $m_{\tilde{t}_j}$ denoting the pole masses; (ii) The renormalized (real) mixing angle $\tilde{\theta}$ is defined by requiring the real part of the off-diagonal elements $D_{\text{ren},12}(Q^2)$ and $D_{\text{ren},21}(Q^2)$ to vanish. Thus, for the fixed scale Q^2 the [virtual/real] particles $\tilde{t}_1$ and $\tilde{t}_2$ propagate independently of each other and do not oscillate.

The so-obtained (running) mixing angle depends on the renormalization point Q, which we will indicate by writing $\tilde{\theta}(Q^2)$. The appropriate choice of Q depends on the characteristic scale of the observable that is analyzed. The real shift connecting two different values of the renormalization point is given by the renormalization group. At NLO SUSY-QCD we have $\delta\tilde{\theta}(Q^2) = \text{Re}\,\Sigma_{12}(Q^2)/[m^2_{\tilde{t}_1} - m^2_{\tilde{t}_2}]$, leading to a finite shift

$$\tilde{\theta}(Q_1^2) - \tilde{\theta}(Q_2^2) = \frac{4\alpha_s m_{\tilde{g}} m_t \cos(2\tilde{\theta})}{3\pi(m^2_{\tilde{t}_2} - m^2_{\tilde{t}_1})}\,\text{Re}\big[B_0(Q_2^2, m_{\tilde{g}}, m_t) - B_0(Q_1^2, m_{\tilde{g}}, m_t)\big] \quad (5)$$

where the function B_0 is the usual two-point function with the integration measure $d^n k/(i\pi^2)$. As a noteworthy consequence of the running-mixing-angle scheme, we mention that some LO symmetries of the Lagrangean are retained in the NLO observables. For instance, if for only one kind of external stop particle one chooses $Q = m_{\tilde{t}}$, the results for the other stop particle can be derived by a simple operation. Amongst others, this operation involves the interchange of the two stop masses in all expressions, including the argument of the running mixing angle.

When dealing with virtual stop states with arbitrary p^2, the off-diagonal elements of the propagator matrix can be absorbed into a redefinition of the mixing of the stop fields, described by an effective (complex) running mixing angle $\tilde{\theta}_{\text{eff}}(p^2) \equiv \tilde{\theta}_0 - \delta\tilde{\theta}_{\text{eff}}(p^2)$. This generalization amounts to a diagonalization of the complex symmetric stop propagator matrix D_{ren}, including the full self-energy $\Sigma(p^2)$, by a complex orthogonal matrix $\mathcal{R}(\delta\tilde{\theta}_{\text{eff}})$. The so-defined effective running mixing angle is given by

$$\tilde{\theta}_{\text{eff}}(p^2) = \tilde{\theta}_0 - \frac{1}{2}\arctan\left[\frac{2\,\Sigma_{12}(p^2)}{m^2_{\tilde{t}_1} - m^2_{\tilde{t}_2} + \Sigma_{22}(p^2) - \Sigma_{11}(p^2)}\right] \xrightarrow{\text{NLO}} \tilde{\theta}(p^2) + \frac{\text{Im}\,\Sigma_{12}(p^2)}{m^2_{\tilde{t}_2} - m^2_{\tilde{t}_1}} \quad (6)$$

From this point of view the use of a diagonal Breit–Wigner propagator matrix is straightforward. For instance, in the toy process $t\tilde{g} \to t\tilde{g}$ all NLO stop-mixing contributions to the virtual stop exchange can be absorbed by introducing the effective mixing angle in the LO matrix elements. The argument of this effective mixing angle is given by the virtuality of the exchanged stop particles.

This procedure also applies to multiscale processes like $q\bar{q} \to t\bar{t}_i\tilde{g}$ or $e^+e^- \to \tilde{t}_1\bar{\tilde{t}}_2$, where the effective $g\tilde{t}_1\bar{\tilde{t}}_2/\gamma\tilde{t}_1\bar{\tilde{t}}_2$ couplings become non-zero due to the different scales of the redefined stop fields.

3 Decays in the Stop Sector and Hadroproduction of Stop Pairs

As explicit examples of processes that involve the mixing-angle renormalization, we mention the decay widths in the stop sector [5,7]. The corresponding LO expressions depend on the mixing angle, which therefore has to be renormalized. For instance, at LO the strong-interaction stop and gluino decays read

$$\begin{aligned} \Gamma_{LO}[\tilde{t}_{1,2} \to t\,\tilde{g}] &= \frac{2\alpha_s\kappa}{3m^3_{\tilde{t}_{1,2}}}\left[m^2_{\tilde{t}_{1,2}} - m_t^2 - m_{\tilde{g}}^2 \pm 2m_t m_{\tilde{g}}\sin(2\tilde{\theta})\right] \\ \Gamma_{LO}[\tilde{g} \to \bar{t}\,\tilde{t}_{1,2}] &= -\frac{\alpha_s\kappa}{8m^3_{\tilde{g}}}\left[m^2_{\tilde{t}_{1,2}} - m_t^2 - m_{\tilde{g}}^2 \pm 2m_t m_{\tilde{g}}\sin(2\tilde{\theta})\right] \end{aligned} \tag{7}$$

where $\kappa = [(m^2_{\tilde{t}_{1,2}} - m_t^2 - m_{\tilde{g}}^2)^2 - 4m_t^2 m_{\tilde{g}}^2]^{1/2}$ is the usual 2-particle phase-space factor. The NLO SUSY-QCD corrections are relatively small for the weak-interaction decay modes, like the decay of a stop particle to a neutralino or a chargino. They are larger and positive (negative) for the strong-interaction decay of a stop (gluino) to a top quark. The dependence of the corresponding K factors (Γ_{NLO}/Γ_{LO}) on the mixing angle is rather weak. This implies an in general even weaker dependence on the definition of the mixing angle in different renormalization schemes.

At hadron colliders, diagonal pairs of stop particles can be produced at lowest order SUSY-QCD in quark–antiquark annihilation and gluon–gluon fusion [8]: $q\bar{q}/gg \to \tilde{t}_j\bar{\tilde{t}}_j$ $(j = 1,2)$. Mixed pairs $\tilde{t}_1\bar{\tilde{t}}_2$ and $\tilde{t}_2\bar{\tilde{t}}_1$ cannot be produced in lowest order since the $g\tilde{t}\bar{\tilde{t}}$ and $gg\tilde{t}\bar{\tilde{t}}$ vertices are diagonal in the chiral as well as in the mass basis. Introducing the partonic energy $\sqrt{s}$ and the velocity $\beta_j = (1 - 4m^2_{\tilde{t}_j}/s)^{1/2}$, the LO partonic cross sections may be written as

$$\begin{aligned} \hat{\sigma}_{LO}[q\bar{q} \to \tilde{t}_j\bar{\tilde{t}}_j] &= \frac{\alpha_s^2\pi}{s}\,\frac{2}{27}\,\beta_j^3 \\ \hat{\sigma}_{LO}[gg \to \tilde{t}_j\bar{\tilde{t}}_j] &= \frac{\alpha_s^2\pi}{s}\left\{\beta_j\left(\frac{5}{48}+\frac{31m^2_{\tilde{t}_j}}{24s}\right) + \left(\frac{2m^2_{\tilde{t}_j}}{3s}+\frac{m^4_{\tilde{t}_j}}{6s^2}\right)\log\left(\frac{1-\beta_j}{1+\beta_j}\right)\right\} \end{aligned} \tag{8}$$

These LO expressions coincide with the ones for light-flavor squarks in the limit of large gluino masses [9]. The hadronic $p\bar{p}/pp$ cross sections are obtained by folding the partonic cross sections with $q\bar{q}$ and gg luminosities. At the Tevatron the dominant mechanism for large stop masses is the valence $q\bar{q}$ annihilation. At the LHC the gluon-fusion mechanism plays a more prominent role.

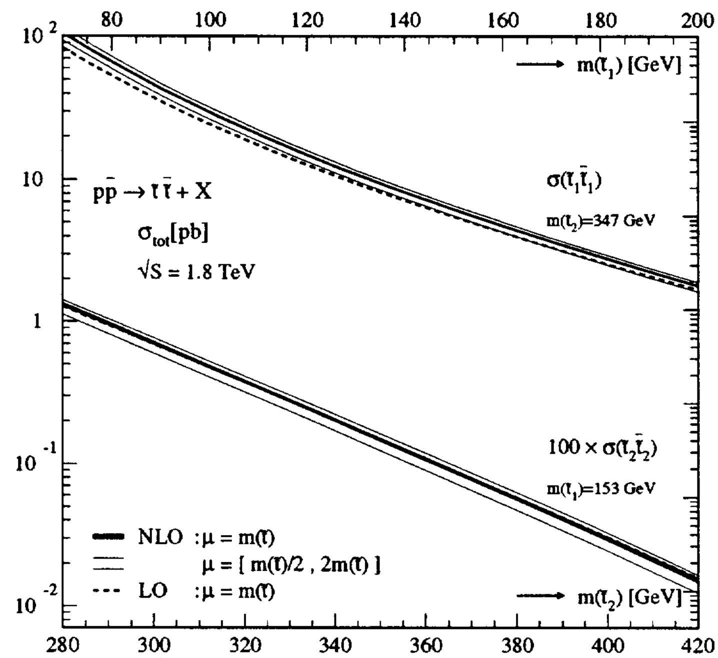

Figure 1: The total cross sections for $p\bar{p} \to \tilde{t}_1\bar{\tilde{t}}_1$ (upper half) and $p\bar{p} \to \tilde{t}_2\bar{\tilde{t}}_2$ (lower half) at the Tevatron as a function of $m_{\tilde{t}}$. The band for the NLO result indicates the uncertainty due to the renormalization/factorization scale $\mu = \mu_R = \mu_F$. The input parameters are chosen as $m_t = 175$ GeV, $m_{\tilde{q}} = 256$ GeV, $\sin 2\tilde{\theta} = -0.99$, and $m_{\tilde{g}} = 284$ GeV. The line-thickness of the NLO curves represents the simultaneous variation of the gluino mass between 200 (284) and 800 GeV for $\tilde{t}_1$ ($\tilde{t}_2$)-pair production and the variation of $\sin(2\tilde{\theta})$ over its full range. We have adopted the CTEQ4M parametrization[10] of the parton densities.

In Fig. 1 we present the total cross section for $\tilde{t}_j\bar{\tilde{t}}_j$ production at the Tevatron. For a consistent comparison of LO and NLO results, we calculate all quantities [$\alpha_s(\mu_R^2)$, the parton densities, and the partonic cross sections] in LO and NLO, respectively. The NLO SUSY-QCD corrections stabilize the theoretical predictions considerably, reducing the large LO scale dependence to a mere 30% in the interval $m_{\tilde{t}_j}/2 < \mu < 2m_{\tilde{t}_j}$. The total cross sections play a crucial role in the experimental analyses. They either serve to extract the exclusion limits for the mass parameters from the data, or, in the case of discovery, they can be exploited to determine the masses of the stop particles.[a] All this is facilitated by the fact that the cross sections depend essentially only on the masses of the produced stop particles, and very little on the other supersymmetric parameters, i.e. the gluino mass, the masses of the light-flavor squarks and the mixing angle. In Fig. 1 this is exemplified by the variation of the cross section with the gluino mass and the mixing angle, as indicated by the thick NLO curves. Note that this feature also holds at the LHC.

In the mass range considered, the SUSY-QCD corrections are small (and negative) for a dominant $q\bar{q}$ initial state. If, in contrast, the gg initial state dominates, the corrections are positive and reach a level of 30–40%. The relatively large mass dependence of the K factor for $\tilde{t}_1\bar{\tilde{t}}_1$ production at the Tevatron, shown in Fig. 1, can therefore be attributed to the fact that the gg initial state is important for small $m_{\tilde{t}_1}$, whereas the $q\bar{q}$ initial state dominates for large $m_{\tilde{t}_1}$. The relative contribution from the gg initial state is larger than observed for the production of light-flavor squarks [9], where the LO gluino-exchange contribution dominates the threshold behavior. This gluino-exchange contribution is absent for stop-pair production.

In $p\bar{p}/pp$ collisions, the production cross sections for non-diagonal final states, $\tilde{t}_1\bar{\tilde{t}}_2$ and $\tilde{t}_2\bar{\tilde{t}}_1$, are of order α_s^4. They exhibit a strong dependence on the mixing angle [$\propto \sin^2(4\tilde{\theta})$], which would allow the measurement of the mixing angle in hadron collisions. However, the production rates are suppressed by four to five orders of magnitude with respect to the ones for $\tilde{t}_2\bar{\tilde{t}}_2$ production.

Acknowledgments

We are grateful to Michael Plümacher and the authors of Ref. [7] for valuable discussions on the mixing angle and its renormalization. W.B. acknowledges the support by a fellowship of the Royal Dutch Academy of Arts and Sciences.

References

1. J. Ellis and S. Rudaz, *Phys. Lett.* B **128**, 248 (1983).
2. K. Ackerstaff *et al.*, Opal Coll., *Z. Phys.* C **75**, 409 (1997); R. Barate *et al.*, Aleph Coll., CERN-PPE/97-084 [hep-ex/9708013].
3. S. Abachi *et al.*, D0 Coll., *Phys. Rev. Lett.* **76**, 2222 (1996).
4. A. Bartl *et al.*, in *'e^+e^- Collisions at TeV Energies: The Physics Potential'*, ed. P.M. Zerwas, DESY 96-123D; E. Accomando *et al.*, hep-ph/9705442.
5. W. Beenakker *et al.*, *Z. Phys.* C **75**, 349 (1997).

[a]In a scenario with a stable LSP the masses cannot easily be reconstructed directly.

6. M.A. Diaz, Proceedings of the Meeting of the American Physical Society, Albuquerque, DPF Conf. 1994.
7. S. Kraml *et al.*, *Phys. Lett.* B **386**, 175 (1996); A. Djouadi *et al.*, *Phys. Rev.* D **55**, 6975 (1997).
8. W. Beenakker *et al.*, CERN-TH/97-177 [hep-ph/9710451].
9. W. Beenakker *et al.*, *Phys. Rev. Lett.* **74**, 2905 (1995), *Z. Phys.* C **69**, 163 (1995), *Nucl. Phys.* B **492**, 51 (1997).
10. H.L. Lai *et al.*, *Phys. Rev.* D **55**, 1280 (1997).